

# THE DISTANCE, INCLINATION, AND SPIN OF THE BLACK HOLE MICROQUASAR H1743–322

JAMES F. STEINER<sup>1</sup>, JEFFREY E. MCCLINTOCK<sup>1</sup>, AND MARK J. REID<sup>1</sup>

*Draft version March 16, 2019*

## ABSTRACT

During its 2003 outburst, the black-hole X-ray transient H1743–322 produced two-sided radio and X-ray jets. Applying a simple and symmetric kinematic model to the trajectories of these jets, we determine the source distance,  $8.5 \pm 0.8$  kpc, and the inclination angle of the jets,  $75^\circ \pm 3^\circ$ . Using these values, we estimate the spin of the black hole by fitting its *RXTE* spectra, obtained during the 2003 outburst, to a standard relativistic accretion-disk model. For its spin, we find  $a_* = 0.56^{+0.16}_{-0.46}$  (68% limits);  $-0.23 < a_* < 0.83$  at 90% confidence. We rule strongly against an extreme value of spin:  $a_* < 0.95$  at 99.7% confidence. Our result, which depends on an empirical distribution of black hole masses, takes into account all known sources of measurement error.

*Subject headings:* black hole physics — stars: individual (H1743–322) — X-rays: binaries

## 1. INTRODUCTION

About 50 stellar-mass black holes have been discovered and about two dozen of these have been well studied at optical or radio wavelengths (Remillard & McClintock 2006; Özel et al. 2010). They are all accretion-powered X-ray sources located in X-ray binary systems. In each system, the X-ray source is fueled by gas that feeds from a mass-donor star into the black hole’s accretion disk. Within a few hundred kilometers of the black hole, the gas reaches a temperature of  $\sim 10^7$  K and produces a luminosity that can approach the Eddington limit ( $\sim 10^{39}$  erg s<sup>-1</sup>). More than 80% of such sources are transient, with outbursts lasting a year or so followed by years or decades of quiescence. Typically, the host binaries have short orbital periods ( $P \sim 1$  day) and are comprised of a low-mass ( $\lesssim 1 M_\odot$ ) secondary star and a  $\sim 10 M_\odot$  black hole. Presently, neither the masses nor the orbital period of our featured system, H1743–322, are known. Nevertheless, as we now describe, the wealth of data available for H1743–322 (hereafter H1743) strongly indicates that it is a typical short-period black hole transient.

Studies of X-ray spectral and timing data leave little doubt that H1743 contains a black hole primary (Kalemci et al. 2006; McClintock et al. 2009; Motta et al. 2010), notwithstanding the lack of dynamical evidence. While large outbursts of H1743 occurred in 1977, 2003 and 2008, our focus here is on the major 2003 outburst. During this 9-month active period, H1743 was observed 170 times using the PCA and HEXTE detectors aboard the *Rossi X-ray Timing Explorer (RXTE)* (McClintock et al. 2009). The source exhibited two distinct phases of evolution: (1) During the first three months (when the source was observed on an almost daily basis) H1743 flared continually and violently and was in the steep power-law (SPL) or intermediate (SPL:Hard) state (see Remillard & McClintock for discussion of these X-ray states). On the 47th day of outburst (MJD 52766), an event of central importance occurred – the radio/X-

ray jets we model were launched during an intense power-law flare (discussed below). (2) During the next four months, the source was locked in the thermal dominant (TD) state, and the source intensity decayed smoothly and monotonically. It is primarily these TD-state data that we use to determine the spin of H1743.

An important X-ray timing result derived from the 2003 outburst was the discovery of a pair of quasi-periodic oscillations (QPOs) at 240 Hz and 165 Hz (Homan et al. 2005; Remillard et al. 2006). Similar high-frequency (HF) QPOs with a commensurate frequency ratio of 3:2 are seen for three other dynamically-confirmed black holes (XTE J1550–564, GRO J1655–40 and GRS 1915+105).

About one year after the onset of the 2003 outburst, bipolar X-ray jets were discovered and observed a total of three times using *Chandra* (Corbel et al. 2005). Radio observations, which commenced several months before the X-ray observations, resulted in four detections of the eastern jet (only), followed about two months later by a single detection of the western jet (Corbel et al. 2005). Large-scale X-ray jets are rare, having been previously observed for only one other microquasar, namely XTE J1550–564, which is similar in many respects to H1743 (for comparisons, see McClintock et al. 2009). In its 1998 outburst, XTE J1550–564 produced relativistic jets at early times whose launch date was unambiguously tied to the occurrence of a remarkable X-ray flare (Hannikainen et al. 2009; Steiner & McClintock 2011).

H1743’s X-flare on MJD 52766 showed many similarities to the flare from XTE J1550–564; a comparison is shown in Figure 12 of McClintock et al. (2009). Additionally, we note that both flares occurred during a dip in the X-ray rms power (0.1–10 Hz), a jump in frequency of the low-frequency QPOs, and at the time of onset of the high-frequency QPOs (Sobczak et al. 2000; Remillard et al. 2006). The similar behavior of these two sources, and the coincidence for XTE J1550–564 between the X-ray flare and the launch date of the jet, motivated us to search the VLA archive for additional observations of H1743. This search was fruitful, and in Section 2 we report three additional radio jet detections at early times that link the jets to the 2003 X-ray flare.

jsteiner@cfa.harvard.edu

<sup>1</sup>Harvard-Smithsonian Center for Astrophysics, 60 Garden Street, Cambridge, MA 02138.

To deduce the source distance and jet inclination angle of H1743 we model the proper-motion data derived from the X-ray and radio observations. In doing so, we closely follow our recent study of the large-scale X-ray/radio jets of XTE J1550–564 (Steiner & McClintock 2011), which builds on the pioneering work of Wang et al. (2003) and Hao & Zhang (2009). Using a model originally applied to gamma-ray bursts, we concluded that XTE J1550–564 is embedded in a pc-scale cavity in which the jets move relatively unimpeded until they impact the cavity walls, thereby decelerating the jets and producing shock emission. The circumstances in the case of H1743 are very similar, and herein we apply this same model to obtain constraints on the distance and jet inclination angle (presumed to be the inclination of the spin axis; see Steiner & McClintock 2011).

The evolution of H1743’s jets have already been studied by Hao & Zhang (2009); however, our aims differ from theirs. They were primarily interested in the environment of the black hole. While assuming an earlier launch date for the jets, they adopted the nominal values of distance and inclination ( $D = 8$  kpc and  $i = 73^\circ$ ) suggested by Corbel et al. (2005). Our attention is focused on deriving accurate constraints on  $D$  and  $i$  for H1743, which we use in turn to constrain the spin of the black hole<sup>2</sup>.

We estimate the spin of H1743 using the continuum-fitting (CF) method, which so far has been used to measure the spins of nine stellar-mass black holes (McClintock et al. 2011; Gou et al. 2011). In the CF method, one estimates the inner radius of the accretion disk  $R_{\text{in}}$ , which is identified with the radius of the innermost stable circular orbit  $R_{\text{ISCO}}$ . Knowing both  $R_{\text{ISCO}}$  and  $M$  is equivalent to knowing the spin parameter  $a_*$  because  $R_{\text{ISCO}}/M$  is a monotonic function of  $a_*$ , decreasing from 6 to 1 as the spin parameter increases from 0 to 1 (Bardeen et al. 1972; we herein adopt  $c = G = 1$ ). In the CF method, one determines  $R_{\text{ISCO}}$  by modeling the X-ray continuum spectrum of the dominant thermal component using a fully relativistic model of a thin accretion disk. The observables are X-ray flux, temperature, distance  $D$ , inclination  $i$ , and mass  $M$ . In order to obtain reliable values of  $a_*$ , it is essential to select X-ray spectra that have a strong thermal component and to have accurate estimates of  $D$ ,  $i$  and  $M$ . For H1743, we use our jet model to determine the first two parameters, and we estimate  $M$  using the known distribution of black hole masses for X-ray transient sources.

## 2. DATA

To search for the presence of radio jets near the time of their expected production (Section 1), we examined high spatial resolution A-configuration VLA images taken early during H1743’s 2003 outburst (see McClintock et al. 2009). Calibrated data from the VLA archive for MJD 52779.4, 52782.4, and 52786.4 were imaged using the Astronomical Image Processing System (AIPS) task IMAGR. The source was detected at 8.4 and 14.9 GHz, but here we only use the 14.9 GHz data, which had sufficient angular resolution to clearly resolve source

components. The synthesized beam was approximately  $0.6''$  by  $0.2''$  elongated north-south. Fortunately, the jet position angle is almost exactly east-west (Corbel et al. 2005), allowing us to identify components separated by about  $\gtrsim 0.2''$ . At all three epochs, the source displayed a dominant component and a weak component offset towards the west. At MJD 52779.4, just 13 days after H1743’s X-ray flare, their separation was  $166 \pm 20$  mas. Later, on MJD 52782.4 and MJD 52786.4 the separations were  $256 \pm 20$  mas and  $288 \pm 20$  mas, respectively.

The majority of jet data considered in our analysis are taken from Tables 1 and 3 of Corbel et al. (2005). These tables provide jet-source separation measurements for radio and X-ray observations which were conducted 6 months and later following H1743’s jet-launching flare. The X-ray data consist of three *Chandra* X-ray observations. Both jets were detected in each  $\sim 30$  ks image. In radio, Corbel et al. (2005) report five detections from the Australian Telescope Compact Array (ATCA). The eastern jet was present in each image, but the western jet was detected only once, in the final observation. (Neither jet was detected in two subsequent ATCA observations.) All of the X-ray and radio observations were carried out between MJD 52955 and MJD 53092, when the jet-source separations were in the range  $\sim 4'' - 7''$ . The substantially larger angular separations of the eastern jet indicate that it is approaching and the western jet is receding.

In determining the spin of H1743, we analyze the full set of *RXTE* PCU-2 “standard 2” data obtained during the 2003 outburst, with the spectra binned into 170 half-day intervals. These spectra have been modeled in detail by McClintock et al. (2009) and Steiner et al. (2009), and we use the same data reduction procedures here. Briefly, all the data are dead-time corrected, background subtracted, and analyzed with the inclusion of a 1% systematic uncertainty (Jahoda et al. 2006). We standardize all detector calibrations to the Toor & Seward (1974) values for the Crab using a custom model which adjusts both the overall flux normalization and the spectral shape (see Steiner et al. 2010). During the early weeks of the outburst cycle, *RXTE*’s pointing was offset by  $0.32^\circ$  from H1743. We have corrected the fluxes to the full collimator transmission by assuming a triangular response with  $\text{FWHM} = 1^\circ$  (see Steiner et al. 2009).

## 3. THE BALLISTIC JETS: MODEL AND RESULTS

Our jet model, which is based on one developed by Wang et al. (2003), was first applied in describing gamma-ray-bursts. Here, we consider a pair of symmetric jets, each ejected with an initial kinetic energy  $E_0$  and Lorentz factor  $\Gamma_0$ . During their expansion, the jets decelerate as they sweep up gas in their path. Assuming adiabatic expansion, the evolution of the jets is governed by:

$$E_0 = (\Gamma - 1)M_0c^2 + \sigma(\Gamma_{\text{sh}}^2 - 1)m_{\text{sw}}c^2, \quad (1)$$

where  $\Gamma$  is the bulk Lorentz factor of the jet,  $M_0$  the mass of the ejecta,  $\sigma$  is a numerical factor of order unity<sup>3</sup>, and  $\Gamma_{\text{sh}}$  is the Lorentz factor of randomly accelerated

<sup>2</sup> We express black hole spin in the customary way as the dimensionless quantity  $a_* \equiv cJ/GM^2$  with  $|a_*| \leq 1$ , where  $M$  and  $J$  are respectively the black hole mass and angular momentum.

<sup>3</sup>  $\sigma$  ranges from 0.35 in the ultrarelativistic limit to 0.73 in the nonrelativistic limit. For additional details concerning our model, see Steiner & McClintock (2011).

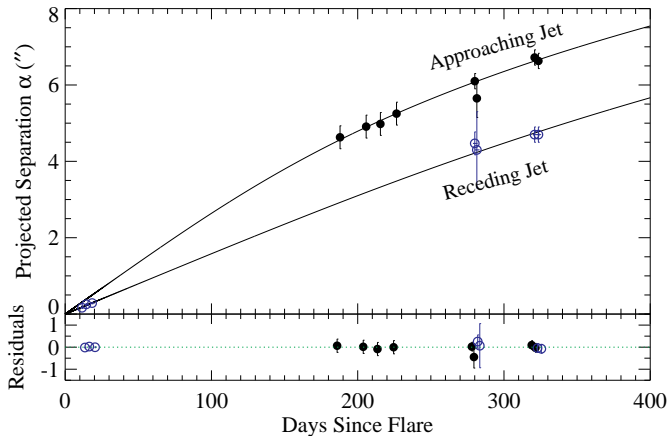


FIG. 1.— Our best fit model for the motion of H1743’s radio and X-ray jets. The eastern jet is denoted by filled circles and the western jet by open circles. For clarity, fit residuals are shown in the bottom panel using a slight offset in time between eastern and western jets.

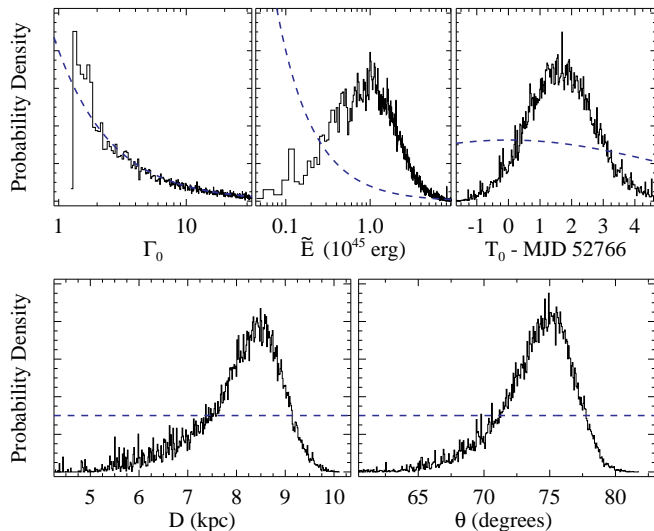


FIG. 2.— MCMC results for the kinematic model. Marginalized probability densities are shown to arbitrary scale for the fit parameters. For reference, the prior for each parameter is indicated by a dashed line.  $\Gamma_0$  is unconstrained at large values, as it was for XTE J1550–564 (Steiner & McClintock 2011). However, the other parameters show little dependence on their priors.

particles at the shock front. The entrained mass,  $m_{sw}$ , is given by  $m_{sw} = \Theta^2 m_p n \pi R^3 / 3$ , where  $\Theta$  is the jet half opening angle,  $n$  the gas density,  $m_p$  is the mass of a proton, and  $R$  the distance traveled by the jet.

We evolve Eqn. 1 in 2-hour time steps, using the inclination of the jet axis to the observer’s line of sight ( $\theta$ ) to calculate the projected separation ( $\delta$ ) between each jet and the central source:  $\delta(t') = R(t) \sin \theta / D$ . Here,  $t' = t \pm R(t) \cos \theta / c$  is the observer’s time, which takes into account for each jet the time delay between H1743’s rest frame and the frame of the observer.

Our full model requires just five parameters:  $D$ ,  $\theta$ ,  $\Gamma_0$ , the launch date  $T_0$ , and  $\tilde{E}$ , the effective energy<sup>4</sup>. Be-

<sup>4</sup>  $\tilde{E} \equiv E_0 (n / 10^{-2} \text{cm}^{-3})^{-1} (\Theta / 1^\circ)^{-2}$ . Following our approach for XTE J1550–564 (Steiner & McClintock 2011), we scale  $\Theta$  and  $n$  using typical values, with density 100 times lower than for the interstellar medium.

cause of the association with the X-ray flare, the prior on the launch date is taken to be  $\text{MJD } 52766 \pm 5$  days; we adopt a flat prior on  $\theta$ ,  $D$ ,  $\log(\Gamma_0)$ , and  $\log(\tilde{E})$ . Our model is fitted via a Markov chain Monte Carlo (MCMC) routine developed using the Metropolis-Hastings algorithm (Hastings 1970) which has been previously applied with this jet model in Steiner & McClintock (2011). The chains are evolved until they are well converged; a total of  $\sim 2 \times 10^5$  chain elements are used<sup>5</sup>.

From the VLA data alone, the identification of the pair of radio sources is ambiguous. We have applied our model by attributing to the two radio sources each allowed combination of eastern jet, western jet, and core. The most probable interpretation is that the two sources correspond to core and western jet emission. The alternative pairings are each ruled out at  $> 97\%$  confidence by our model.

The best fit achieved by the MCMC run is shown in Figure 1 and reaches a goodness of fit  $\chi^2/\nu = 4.9/9 = 0.54$ . Obviously, further modification to the model is not needed<sup>6</sup>. Distributions for the model parameters are shown in Figure 2. Of chief importance, we find that distance and inclination are well constrained:  $D = 8.5 \pm 0.8$  kpc and  $i = 75^\circ \pm 3^\circ$ . The time at which the jets were produced is strongly constrained to  $T_0 = \text{MJD } 52767.6 \pm 1.1$  days, which implies that the jets were launched during or shortly after the X-ray flare event (MJD 52766). Meanwhile, the speed of the jet,  $\Gamma_0$ , has a relatively low maximum a posteriori estimate,  $\Gamma_0 \sim 1.4$ , but is poorly constrained at high values. For the kinematic energy of each jet, we obtain a significant uncertainty of  $\approx 0.5$  dex centered around  $\tilde{E} \approx 10^{45}$  erg. This implies that H1743’s jets are approximately tenfold less energetic than those produced in the 1998 outburst of XTE J1550–564, or alternatively that for H1743 either (1) the density of the surrounding medium is much lower or (2) the jet opening angle is substantially smaller.

#### 4. X-RAY CONTINUUM-FITTING ANALYSIS

We now estimate the spin of the black hole by fitting selected X-ray spectra of H1743. For the three crucial input parameters, we use the values of  $D$  and  $i$  derived in the preceding section and the distribution of black hole masses discussed below. All of our analysis is performed using XSPEC v12.7.0 (Arnaud 1996). Following Steiner et al. (2009) and making minor adjustments, our spectral model has the form  $\text{TBABS}(\text{SIMPL} \otimes \text{KERRBB2})$ , where TBABS and KERRBB2 are respectively the low-energy-absorption and accretion-disk components. The component SIMPL scatters a fraction of the thermal disk photons into a Compton power law. For H1743, this simple convolution model describes only the broad continuum components and is unaffected by the inclusion of weaker features, e.g., warm absorbers or spectral reflection components.

The four free parameters of the spectral model<sup>7</sup> are the (1) fraction of thermal photons  $f_{sc}$  scattered into

<sup>5</sup> Not used in deriving our results were an additional  $\approx 10^5$  links that were generated during a combination of training and burn-in phases.

<sup>6</sup> We have explored the asymmetric models employed for XTE J1550–564 (Steiner & McClintock 2011);  $i$  and  $D$  are unchanged.

<sup>7</sup> Column density  $N_H$  is frozen at  $2.0 \times 10^{22} \text{cm}^{-2}$  (Blum et al. 2009). For KERRBB2, limb darkening and returning radiation are

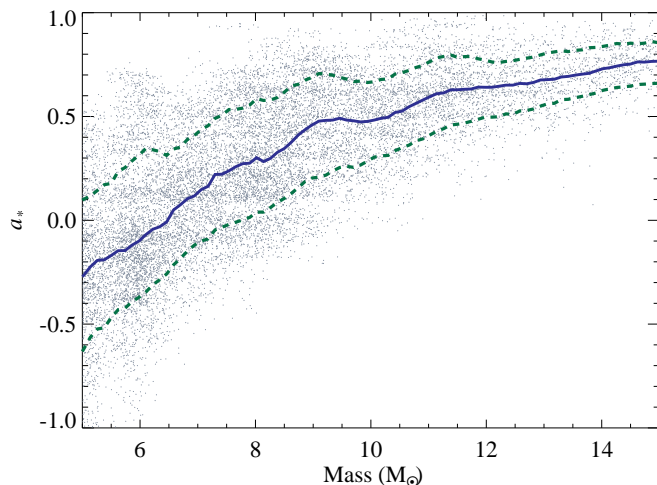


FIG. 3.— The dependence of spin on black hole mass. These estimates incorporate all sources of measurement error. The solid line tracks the average spin at each mass, and the associated 68% confidence interval corresponds to the region between dashed lines.

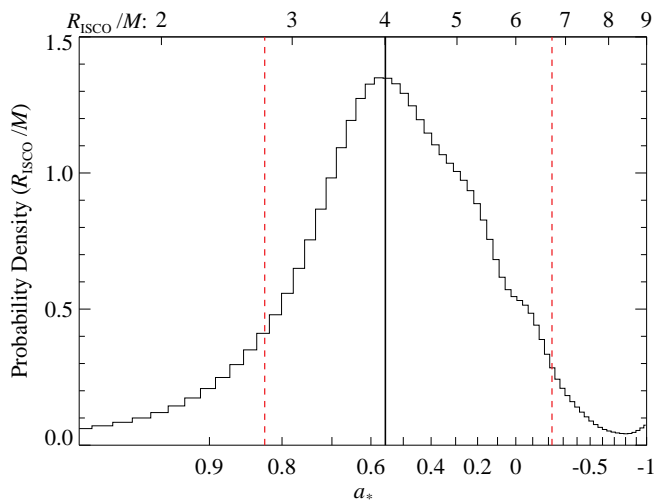


FIG. 4.— Spin probability for the dimensionless measurement variable  $R_{\text{ISCO}}/M$  (top axis) which is uniquely associated with spin (bottom axis). This spin estimate is obtained by assuming a transient black hole mass distribution from Özel et al. (2010). The vertical solid line indicates the maximum likelihood spin, while the 90% confidence range is bounded by dashed lines. These results take into account uncertainties in  $M$ ,  $i$ ,  $D$ ,  $\alpha$  and the absolute X-ray flux calibration. For illustration, the distribution of  $R_{\text{ISCO}}/M$  has been smoothed using a Gaussian kernel with 10% width.

the Compton power law; (2) power-law index  $\Gamma$ ; (3) spin parameter  $a_*$ ; and mass accretion rate  $\dot{M}$ . Mass, inclination, and distance are varied in  $5 \times 10^3$  Monte-Carlo samples, and all 170 spectra are fitted for each setting. The uncertainty in the absolute calibration of the X-ray flux is accounted for by randomly varying the overall flux normalization by 10% for each triplet setting of  $M$ ,  $i$ , and  $D$  (e.g., Steiner et al. 2011). We similarly marginalize over uncertainty in the viscosity parameter  $\alpha$  by randomly assigning either  $\alpha = 0.01$  or  $\alpha = 0.1$  (e.g., King et al. 2007; Pessah et al. 2007), which are two representative values available to our model. Both of these uncertain-

switched on and the torque at the inner boundary is set to zero. For SIMPL, we use the faster upscattering-only option.

ties have a small effect on  $a_*$  compared to our dominant uncertainty, namely, the unknown black hole mass.

For each of the  $5 \times 10^3$  parameter settings, we apply our standard data selection criteria: disk luminosity between 3% and 30% of the Eddington limit; goodness of fit ( $\chi^2/\nu < 2$ ); and a power-law normalization  $f_{\text{SC}} < 25\%$  (Steiner et al. 2009). Typically, about 30 spectra pass this screening. Finally, each of the  $5 \times 10^3$  samples is given a weight according to the mass distribution assumed, and random draws are made from the selected spectra to achieve an estimate of spin. The dependence between the inferred value of spin and the black hole’s mass is illustrated in Figure 3. As mass is varied from  $M = 5M_\odot$  to  $15M_\odot$ , the spin changes from  $a_* \approx -0.25$  to  $a_* \approx 0.75$ .

Recently, Özel et al. (2010) compiled all the dynamical measurements of mass that have been made for black hole transients and determined the following best-fit probability distribution:

$$P(M) = \begin{cases} \text{Exp}[(6.30M_\odot - M)/1.57M_\odot]/1.57M_\odot, & M > 6.3M_\odot, \\ 0, & M \leq 6.3M_\odot. \end{cases} \quad (2)$$

In Figure 4, we use this distribution to estimate the spin of H1743. We find  $a_* = 0.56^{+0.16}_{-0.46}$  (68% confidence interval) with a 90% confidence interval of  $-0.23 < a_* < 0.83$ . From this analysis, we find that an extremal spin  $a_* > 0.95$  is ruled out at  $3\sigma$  confidence. This makes H1743 one of a growing population of black-hole microquasars known to have moderate spin (e.g., A0620–00,  $a_* \approx 0.1$ ; Gou et al. 2011, XTE J1550–564,  $a_* \approx 0.5$ ; Steiner et al. 2011).

## 5. CONCLUSIONS

We have modeled the proper motion of the radio and X-ray jets of H1743 that were launched during an X-ray flare. Based on our purely kinematic model, we obtain firm estimates of the source distance,  $8.5 \pm 0.8$  kpc, and the jet inclination angle,  $75^\circ \pm 3^\circ$ . Using these constraints on  $D$  and  $i$ , we fitted all 170 X-ray spectra collected during the 2003 outburst of H1743, applied our data selection criteria, and derived a relationship between spin and black hole mass. We then constrained the mass of H1743 using an analytic distribution derived for transient systems that are similar to H1743, thereby arriving at our final result:  $a_* = 0.56^{+0.16}_{-0.46}$ ,  $-0.23 < a_* < 0.83$  at 90% confidence. Meanwhile, we rule strongly against an extreme value of spin:  $a_* < 0.95$  at 99.7% confidence.

This is the first successful application of the X-ray continuum-fitting method that does not rely on any dynamical data to place constraints on one or more of the input parameters  $D$ ,  $M$  and  $i$  – even the orbital period of H1743 is presently unknown! Of course, our constraint on  $a_*$  can be tightened once a dynamical estimate of mass has been obtained.

JFS was supported by the Smithsonian Institution Endowment Funds and JEM acknowledges support from NASA grant NNX11AD08G. Computations were performed using the Odyssey cluster which is supported by the FAS Science Division Research Computing Group at Harvard University.

## REFERENCES

- Arnaud, K. A. 1996, in *Astronomical Society of the Pacific Conference Series*, Vol. 101, *Astronomical Data Analysis Software and Systems V*, ed. G. H. Jacoby & J. Barnes, 17
- Bardeen, J. M., Press, W. H., & Teukolsky, S. A. 1972, *ApJ*, 178, 347
- Blum, J. L., Miller, J. M., Fabian, A. C., Miller, M. C., Homan, J., van der Klis, M., Cackett, E. M., & Reis, R. C. 2009, *ApJ*, 706, 60
- Corbel, S., Kaaret, P., Fender, R. P., Tzioumis, A. K., Tomsick, J. A., & Orosz, J. A. 2005, *ApJ*, 632, 504
- Gou, L., et al. 2011, *ApJ*, in press
- Hannikainen, D. C., et al. 2009, *MNRAS*, 397, 569
- Hao, J. F., & Zhang, S. N. 2009, *ApJ*, 702, 1648
- Hastings, W. 1970, *Biometrika*, 97
- Homan, J., Miller, J. M., Wijnands, R., van der Klis, M., Belloni, T., Steeghs, D., & Lewin, W. H. G. 2005, *ApJ*, 623, 383
- Jahoda, K., Markwardt, C. B., Radeva, Y., Rots, A. H., Stark, M. J., Swank, J. H., Strohmayer, T. E., & Zhang, W. 2006, *ApJS*, 163, 401
- Kalemci, E., Tomsick, J. A., Rothschild, R. E., Pottschmidt, K., Corbel, S., & Kaaret, P. 2006, *ApJ*, 639, 340
- King, A. R., Pringle, J. E., & Livio, M. 2007, *MNRAS*, 376, 1740
- McClintock, J. E., et al. 2011, *Classical and Quantum Gravity*, 28, 114009
- McClintock, J. E., Remillard, R. A., Rupen, M. P., Torres, M. A. P., Steeghs, D., Levine, A. M., & Orosz, J. A. 2009, *ApJ*, 698, 1398
- Motta, S., Muñoz-Darias, T., & Belloni, T. 2010, *MNRAS*, 408, 1796
- Özel, F., Psaltis, D., Narayan, R., & McClintock, J. E. 2010, *ApJ*, 725, 1918
- Pessah, M. E., Chan, C.-k., & Psaltis, D. 2007, *ApJ*, 668, L51
- Remillard, R. A., & McClintock, J. E. 2006, *ARA&A*, 44, 49
- Remillard, R. A., McClintock, J. E., Orosz, J. A., & Levine, A. M. 2006, *ApJ*, 637, 1002
- Sobczak, G. J., McClintock, J. E., Remillard, R. A., Cui, W., Levine, A. M., Morgan, E. H., Orosz, J. A., & Bailyn, C. D. 2000, *ApJ*, 531, 537
- Steiner, J. F., & McClintock, J. E. 2011, *ApJ*
- Steiner, J. F., McClintock, J. E., Remillard, R. A., Gou, L., Yamada, S., & Narayan, R. 2010, *ApJ*, 718, L117
- Steiner, J. F., McClintock, J. E., Remillard, R. A., Narayan, R., & Gou, L. J. 2009, *ApJ*, 701, L83
- Steiner, J. F., et al. 2011, *MNRAS*, 416, 941
- Toor, A., & Seward, F. D. 1974, *AJ*, 79, 995
- Wang, X. Y., Dai, Z. G., & Lu, T. 2003, *ApJ*, 592, 347